Asian Journal of Geological Research

1(2): 65-78, 2018; Article no.AJOGER.43364

Geological and Geoelectrical Delineation of Aquifer Systems in Girinya, North Central Nigeria

A. Aghwadje[1*] and C. I. Unuevho[1]

[1]Department of Geology, Federal University of Technology, Minna, Nigeria.

Authors' contributions

This work was carried out in collaboration between both authors. Author AA designed the study, performed the statistical analysis, wrote the protocol and wrote the first draft of the manuscript. Author CIU managed the analyses of the study and managed the literature searches. Both authors read and approved the final manuscript.

Article Information

DOI: 10.9734/AJOGER/2018/43364
Editor(s):
(1) Dr. Mohamed M. El Nady, Department of Exploration, Egyptian Petroleum Research Institute, Egypt.
Reviewers:
(1) Etim Daniel Uko, Rivers State University, Nigeria.
(2) Zengguang Xu, Xi'an University of Technology, China.
(3) Nordiana Mohd Muztaza, Universiti Sains Malaysia (USM), Malaysia.
Complete Peer review History: http://www.sciencedomain.org/review-history/26080

Original Research Article

Received 12 June 2018
Accepted 18 August 2018
Published 03 September 2018

ABSTRACT

Inhabitants of Girinya are unable to access potable water supply. The existing five boreholes were initially productive only during rainy season. They are now totally unproductive. Only three of existing forty-five hand-dug wells yield water all year now. Thus it is expedient to identify areas where groundwater can be sustainably produced from hand-dug wells and boreholes. This was achieved by integrating surface lithological mapping, water level mapping, Vertical Electric Sounding (VES) and 2D geoelectrical tomography techniques. The VES data were interpreted using WINRESIST, while the 2D geoelectrical data were processed and interpreted using RES2DINV. The exposed lithofacies represent Patti Formation and Agbaja Formation. The sandstone facies of the Patti Formation constitutes the unconfined aquifer from which hand-dug wells produce water. The resistivity values and depth to base of the unconfined aquifer ranges from 48 – 227 Ωm, and 12 – 26 m respectively. The resistivity values support the unconfined aquifer's high porosity (0.27- 0.42) and hydraulic conductivity (40.2 m/day). One major groundwater convergence zone and two subsidiary convergence zones were revealed. The confined aquifers are the deeper subsurface sandstone facies of the Patti Formation. The study reveals (i) that the bottom of hand-dug wells is generally

**Corresponding author: E-mail: akpeswadje@yahoo.com;*

shallower than the base of the unconfined aquifer, and (ii) that confined aquifers exist below 70 m. This information is beneficial to Girinya as they can now deepen hand-dug wells to depth below 26 m, and drill boreholes to depth below 70 m for sustainable water yield.

Keywords: Aquifer system; water level elevation; hydraulic conductivity; resistivity sounding; 2D resistivity imaging.

1. INTRODUCTION

Accessibility to fresh water sources is crucial to human communities, because every person needs about 50 litres of water for daily personal use [1]. Nigerians in rural communities obtain water supply for their daily needs from streams and hand-dug wells. Five boreholes drilled for water supply in Girinya initially produced water during the rainy season only. They are now unproductive. The effort of the residents to obtain water from hand-dug have not been rewarding. Thus, it is necessary to identify areas where groundwater can be sustainably produced from hand-dug wells and boreholes. Prospecting for groundwater is essentially a geological problem [2], because the configuration of aquifer systems is determined by the structural disposition of aquifers and aquitards [3]. An aquifer system is a homogenous body of saturated permeable and non-permeable hydrogeologic unit, which acts as water yielding hydraulic unit of a regional extent [4]. Jatau et al. [5] employed combined vertical electrical sounding (VES) and borehole-drilling data to establish groundwater potential of aquifer systems in Abaji, north central Nigeria. Their study revealed that lithostratigraphy controls the structural disposition of aquifer and aquitard units that constitute multi-layered aquifer system. Idris-Nda et al. [6] undertook resistivity surveying and hydrogeological mapping to describe the hydrogeology of the mixed geologic terrain of Niger State. They found that groundwater potential is variable in sedimentary terrain. The electrical resistivity method is one of the most adopted techniques widely employed for groundwater exploration [7,8]. However, Aizebeokhai [9] reported that in areas where subsurface geology is relatively complex and subtle, two-dimensional (2D) electrical resistivity imaging provides a more accurate model of the subsurface resistivity distribution. The VES measures resistivity distribution in one-dimension (1D) and it has inherent limitations because of its inability to discriminate between saturated quartz, clean sands and clayey

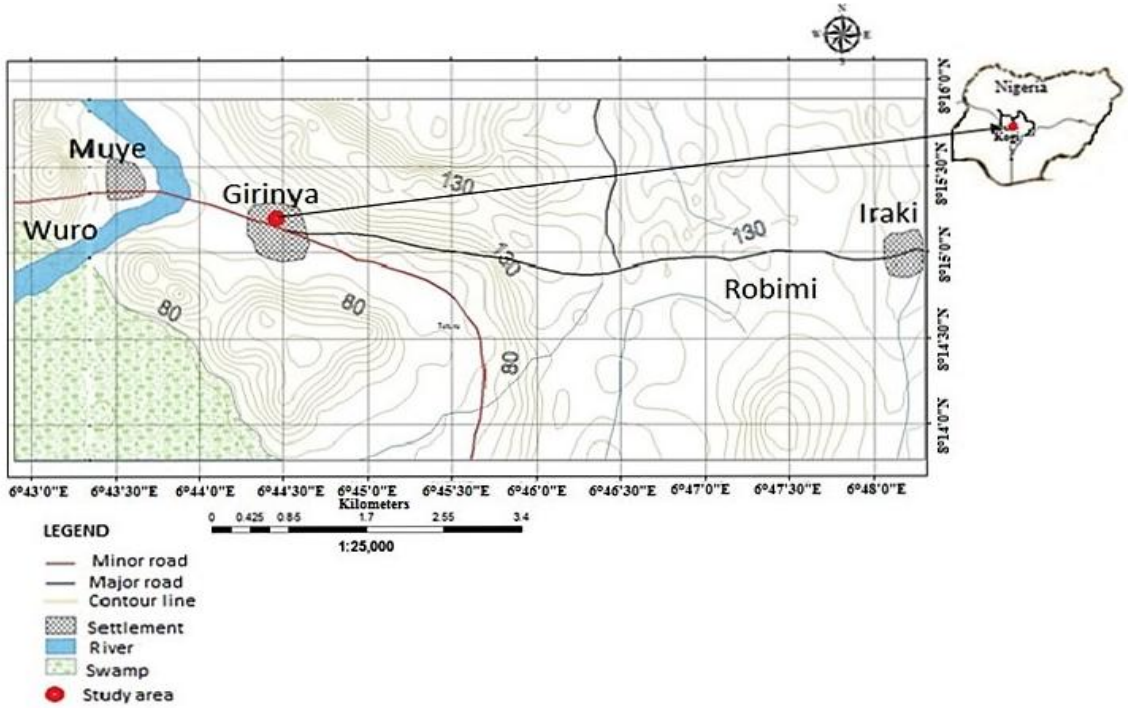

Fig. 1. Location map of the study area

formations as both are characterized by low resistivity values. The induced polarization (IP) combined with resistivity technique is capable of distinguishing clay mineralization from saturated sandy formations. The one-dimensional model of resistivity variation with depth fails to identify water bearing formations between two VES stations simultaneously in a study by Ratnakumari et al. [10]. This present research integrated surface lithological mapping, water level mapping, vertical electrical soundings and 2D geoelectrical resisitivity imaging to characterize aquifer systems in Girinya of north-central Nigeria.

1.1 Location and Regional Geology of Girinya

Girinya, a semi-urban settlement within latitudes 6°13' 54"N to 6°16' 00"N, and longitudes 6°43' 00"E to 6°48' 48"E in Southern Bida Basin, covers a surface area of about 14.8 km^2 (Fig. 1). The Bida Basin is a northwest-southeast trending intracratonic structure that extends from kotongora in the Northern part of Niger State to areas beyond Lokoja in central Nigeria. The origin of the Basin is closely related to the Satonian upheaval, which affected the lower Benue Trough and south-eastern Nigeria [11]. The stratigraphic framework has been divided geographically into northern and southern Bida Basin. The rocks of this formation are Campanian to Maastrictchian in age [12]. The exposed lithologic facies and their petrographic attributes are characteristics of Patti Formation in the southern Bida Basin.

2. METHODOLOGY

Surface lithological mapping was conducted using a topographical map of Girinya of 1:25, 000 scale. Identified surface lithologic units were associated with geological formations on the basis of observed petrographic attributes. Water level measurement were carried out on forty five hand-dug wells in the area using measuring tape and Geographic positioning system (GPS). The water elevation values were contoured using Surfer contouring software to produce elevation map. Sieve analysis was carried out on ten representative samples across the study, to empirically determine the permeability of aquifer units. The empirical formula proposed by Hazen [13], was used for the determination.

The formula is the following:

$$K = Cd_{10}^{\ 2} \quad (1)$$

Where

K = hydraulic conductivity
$d_{10}^{\ 2}$ = effective grain size diameter
C = 1 if k is in cm/s [14]

Porosity function (n) and coefficient of uniformity (U) were derived following [15]:

$$n = 0.255(1+0.83^{U}) \quad (II)$$

2.1 Geoelctrical Aspects

Resistivity and IP data were recorded using ABEM Terrameter (SAS 4000) during 1D resistivity sounding and 2D electrical resistivity imaging. In addition spontaneous potential (SP) was recorded during the VES. The Schlumberger array was employed for VES, using a maximum current electrode spacing of 600 m. A Wenner alpha array, with minimum electrode spacing of 10 m was adopted for the 2D data measurement. The survey traverse is across E-W direction, which is in conformity with the dip directions of outcrops. The maximum spread length is at 500 m and number of data levels is from six to twelve. The 2D apparent resistivity and time domain IP effect were measured concurrently for each traverse. A total of 4 VES and 2D electrical resistivity imaging were conducted.

2.1.1 Data processing and inversion aspects

The observed apparent resistivity datasets for the resistivity soundings were plotted against half-current electrode spacing (AB/2) on a bi-logarithmic graph sheet. An initial geoelectric model was inferred for each VES station from the combination of exposed lithofacies information, resistivity, cummulative resistivity, SP, and IP data. The refined geoelectrical model was generated from the initial one, by computer iteration using a Win-Resist software. The acquired 2D apparent resistivity and chargeability dataset were filtered and inverted concurrently using RES2DINV software [16].

3. RESULTS AND DISCUSSION

The exposed lithofacies comprise of sandstones, mudstones, siltstones, ironstones, kaolinitic claystone and carbonaceous shales. The sandstone facies are medium – coarse, and sometimes pebbly to conglomeritic. Thus they

are poorly sorted. They are massive and show an upward fining character with channel lag deposits on erosional surface at the base of each sandstone facies unit (Plate I and Fig. 2). The sandstone facies caps the Patti Formation. It changes upward into Agbaja Formation through numerous intercalation with sandstone with ironstone and ferruginized mudstone facies (Plate II and Fig. 3). Downwards, the sandstone facies becomes interbedded with mudstone. The field lithological relationship is shown in the produced geological map (Fig. 4). The Agbaja Formation lies on top of the Patti Formation. They strike NE – SW and dip westwards.

3.1 Grain Size Studies

Grain size distribution curves resulting from sieve analysis are presented in Figs. 5 and 6. Porosity and hydraulic Conductivity values computed from Hazen's statistical grain size method are given in table Table 1. The porosity ranges from 0.27 – 0.42. The porosity is slightly higher than 0.02 – 0.35 and median of 0.26 proposed by Allen et al. [17]. This is attributable to components of friable samples with higher than average porosity value. The computed hydraulic conductivity values range from 4.86 to 40.21 m/day. The range is typical of medium to coarse sand and gravel according to the work of Garg [18].

3.1.1 Hydrogeological mapping result

The water level data are presented in Table 2 and Fig. 7. The water level in the hand-dug wells varies from 1.1 to 13.9 m. The elevation, with respect to sea level varies from 73 m to 43 m. The elevation revealed one major convergence zone, two subsidiary convergence zones, and one divergence zone. The hand-dug wells in the vicinity of the divergence zones generally produce water in the rainy season only.

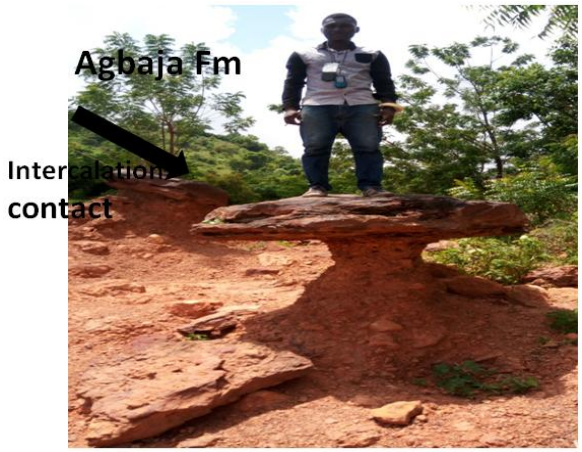

Plate I. Sandstone and ironstone contact

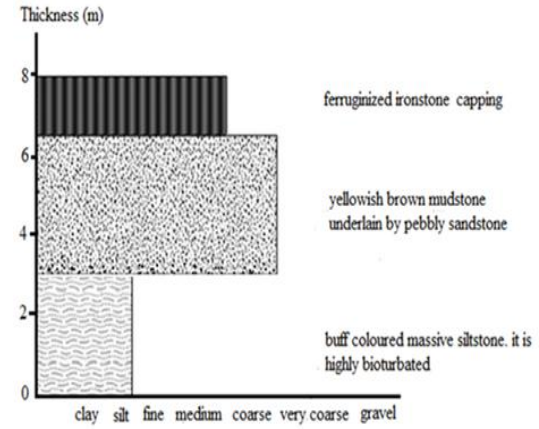

Fig. 2. Lithostratigraphic section

Plate II. Ferruginized mudstone

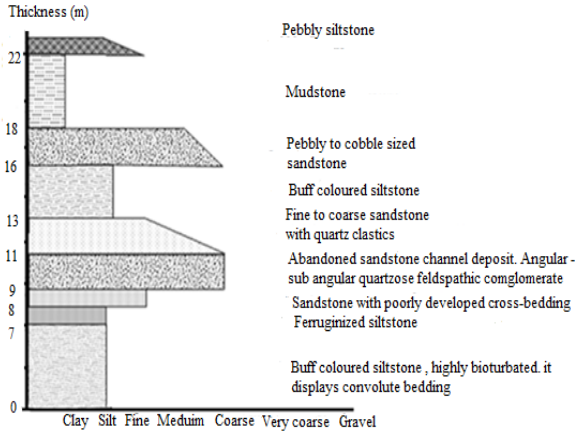

Fig. 3. Lithostratigraphic section

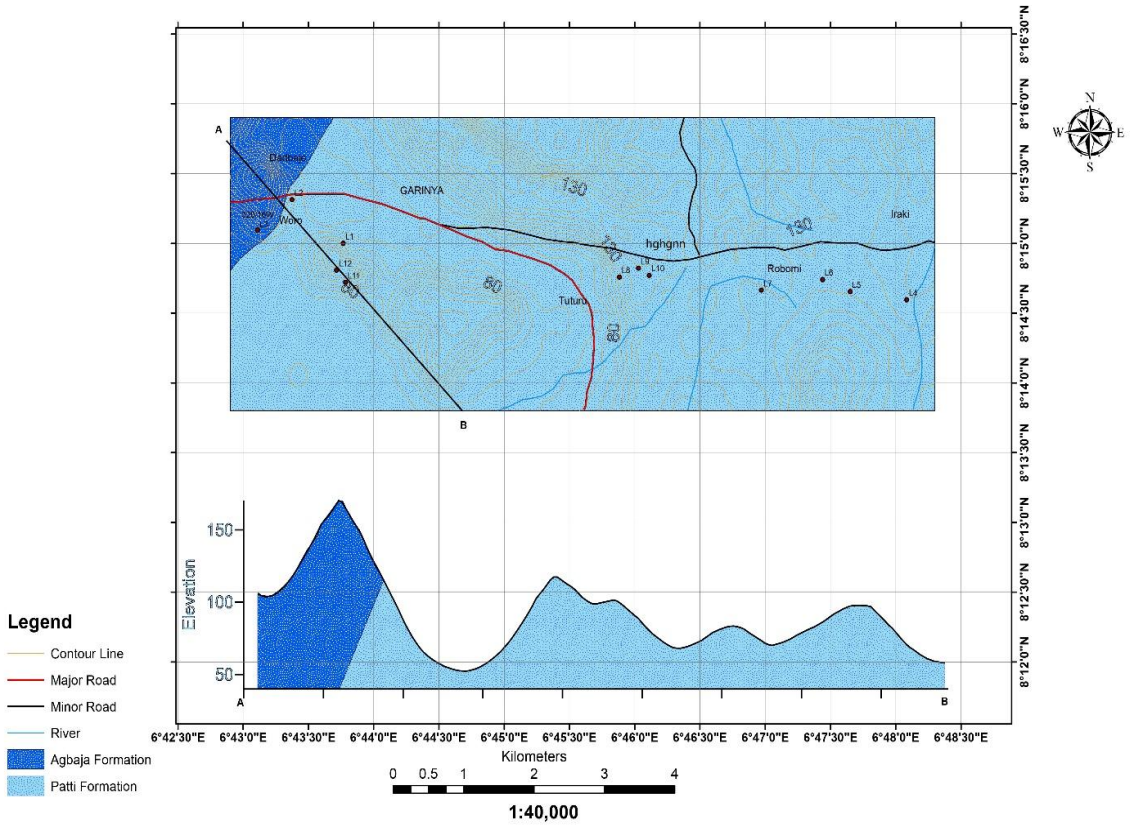

Fig. 4. Geological map and cross section of the area

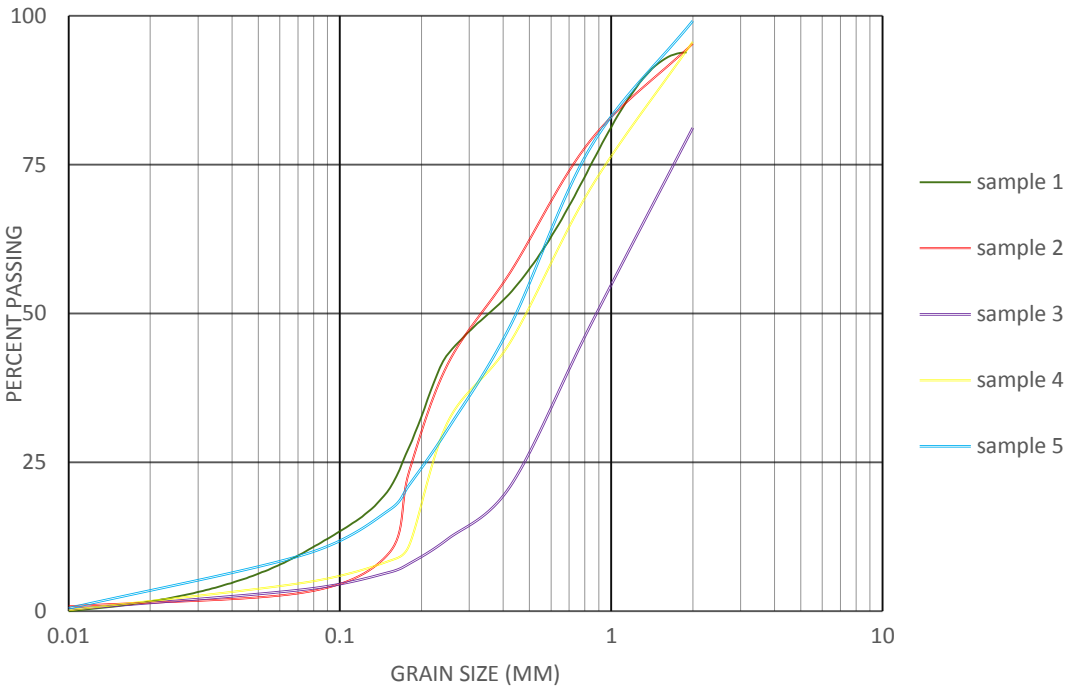

Fig. 5. Grain size distribution curve

Table 1. Soil particle size and hydraulic conductivity values

S/N	Lithology	Coarse sand %	Medium sand %	Fine sand %	Coarse silt %	Fine silt %	D_{10}	D_{60}	μ	η	Hazen (cm/s)	K (m/day)
1	siltstone	5.22	18.91	31.68	33.15	10.05	0.075	0.551	7.34	0.32	5.83×10^{-3}	4.86
2	sandstone	4.69	16.23	37.56	38.34	2.35	0.154	0.497	3.23	0.39	2.46×10^{-2}	20.51
3	sandstone	19.05	33.13	35.63	8.78	3.42	0.216	1.266	5.86	0.34	4.82×10^{-2}	40.21
4	siltstone	4.2	24.78	39.24	26.97	4.68	0.169	0.666	3.93	0.37	2.97×10^{-2}	24.78
5	sandstone	0.85	21.22	47.37	21	9.125	0.084	0.598	7.11	0.32	7.32×10^{-3}	6.1
6	sandstone	3.95	21.83	50.85	17.35	5.33	0.154	0.682	4.41	0.36	2.47×10^{-2}	20.59
7	siltstone	5.95	16.07	39.12	29.99	8.51	0.089	0.578	6.5	0.33	8.16×10^{-3}	6.8
8	sandstone	37.55	23.74	24.34	10.7	2.54	0.207	1.935	9.37	0.29	4.42×10^{-2}	36.86
9	mudstone	32.81	19.61	25.99	14.79	5.85	0.126	1.63	12.99	0.27	1.64×10^{-2}	13.68
10	sandstone	2.49	6.43	29.62	57.14	4.13	0.116	0.247	2.12	0.42	1.41×10^{-2}	11.72

d10= grain-size (mm) corresponding to 10 % by weight passing through the sieves
d60= grain-size (mm) corresponding to 60% by weight passing through the sieves
μ = coefficient of grain uniformity = $\frac{d60}{d10}$
η = Porosity function
K =hydraulic conductivity

Table 2. Well inventory of the study area

Well/ borehole number	Latitude	Longitude	Surface elevation (m)	Water table (m)	Water table elevation (m)	Remarks
1	8.2492	6.7322	75.7	-	-	dry well
2	8.2491	6.7321	67.6	12.7	54.9	
Bh1	8.249	6.7318	70	-	-	non-productive
Bh2	8.2487	6.7321	65.1	-	-	
3	8.2481	6.7327	71.2	11	60.2	dries up during dry season
4	8.2478	6.7326	64.8	12.8	52	
5	8.248	6.7333	77.2	12.4	64.8	seasonally productive
6	8.2487	6.7334	63.4	9.3	54.1	
7	8.2492	6.733	62.7	9.4	52.6	
8	8.2489	6.7325	57.7	10.6	47.1	
9	8.2486	6.7325	56.5	10.5	46	productive throughout the year
10	8.2483	6.732	57.6	10.3	46.8	
11	8.248	6.7321	79.3	10.9	68.4	
12	8.2481	6.731	77.6	13.9	63.7	productive throughout the year
13	8.2486	6.7311	77.6	11.8	65.8	
14	8.2482	6.73	72.7	11.2	61.5	

Well/ borehole number	Latitude	Longitude	Surface elevation (m)	Water table (m)	Water table elevation (m)	Remarks
Bh3	8.2499	6.7301	61.5	-	-	non-productive
15	8.25	6.7307	50.1	7.9	42.2	productive throughout the year
16	8.2496	6.7305	69.7	9	60.7	
17	8.2495	6.7174	80.3	8.8	71.2	seasonally productive
18	8.2504	6.7325	58.6	6.4	52.2	
19	8.251	6.7332	59.4	6.3	53.1	
Bh4	8.2509	6.7336	55.5	-	-	
20	8.2521	6.7345	57.5	2.5	55	
21	8.252	6.7348	58.4	1.96	56.44	
22	8.2526	6.7343	60.3	2.4	57.9	
23	8.2525	44.053	60.3	3.2	57.1	
24	8.2517	6.7343	59.4	4.8	54.6	
25	8.2512	6.7366	57.8	1.6	56.2	
26	8.2507	6.7381	77.2	2.4	74.8	dries up during dry season
27	8.2502	6.7385	56.9	3.1	53.8	productive throughout the year
28	8.2505	6.7391	60.6	3.6	57	
29	8.2501	6.7378	62.1	2.5	59.6	
30	8.2504	6.7376	65.4	2.5	62.9	dries up during dry season
31	8.2495	6.7378	64.5	2.5	62	
32	8.2493	6.7379	58.8	1.86	56.94	
33	8.2493	6.7387	60	2.6	57.6	
34	8.2494	6.7388	58.7	9.5	49.2	
35	8.249	6.739	43.6	2.5	41.1	Productive all year round
36	8.2491	6.7394	62.7	2.5	60.2	
37	8.2496	6.7392	60	3.1	56.9	
38	8.2489	6.7409	53.5	2.2	51.3	
39	8.2492	6.74	59.4	2.4	57	
40	8. 249	6.74	61.8	2.3	59.5	
41	8.2486	6.7405	62.7	1.4	61.3	
42	8.2489	6.7409	62.7	1.8	60.9	
43	8.2487	6.7412	63.6	1.6	62	
44	8.249	6.742	62.7	1.1	61.6	
45	8.2478	6.7398	60.3	2.2	58.1	

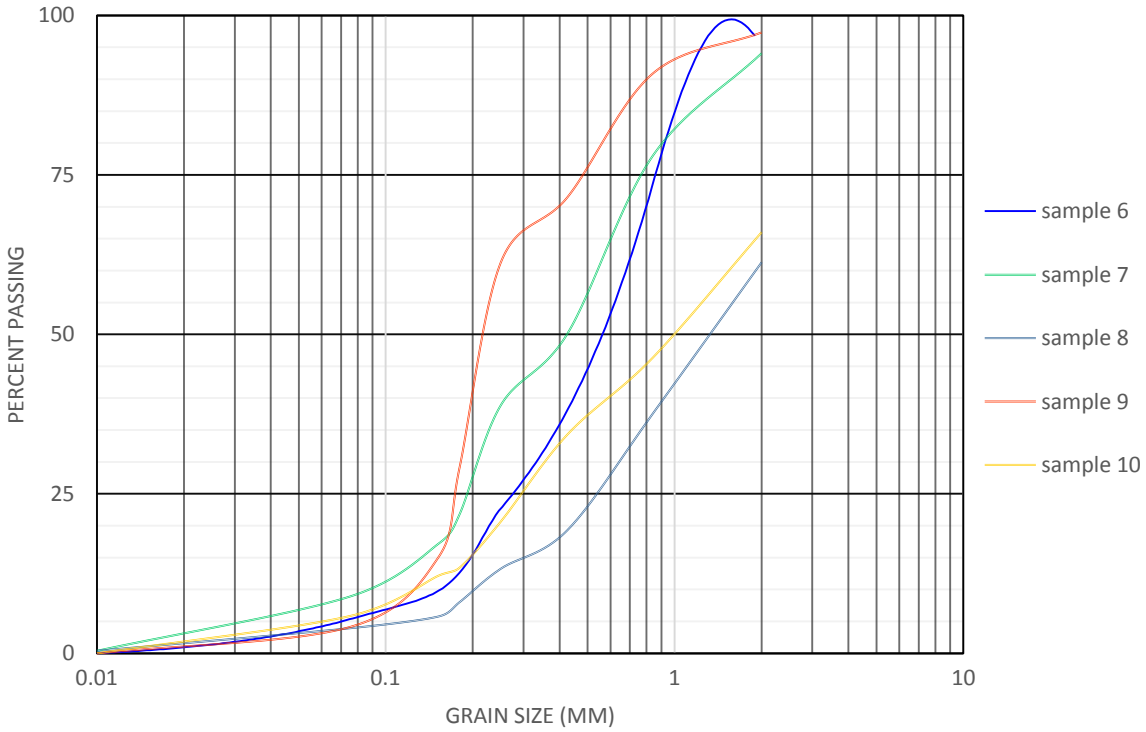

Fig. 6. Grain size distribution curve

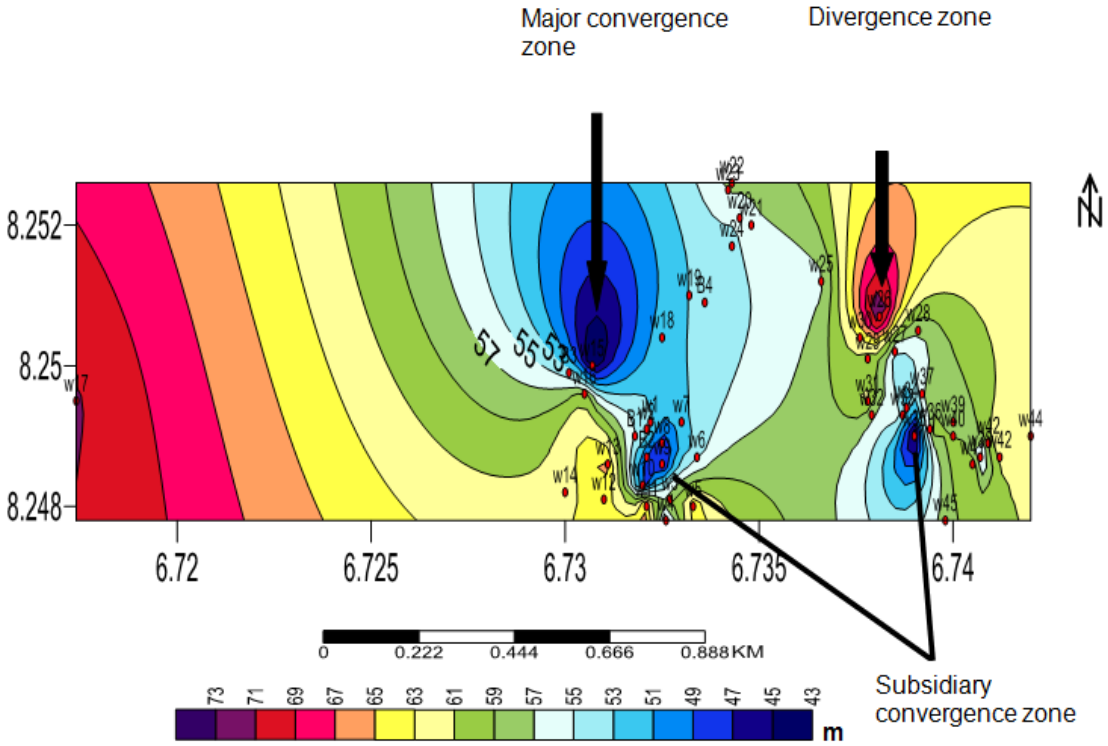

Fig. 7. Water elevation map

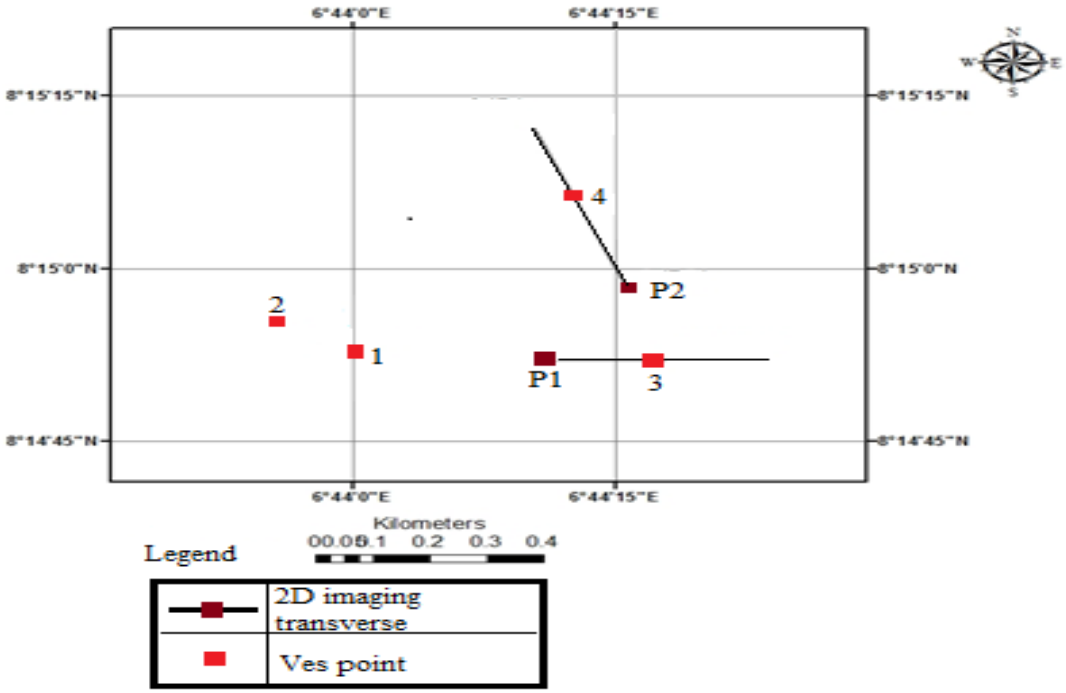

Fig. 8. Geoelectrical sounding stations and 2D traverse

Table 3. Vertical electrical sounding data

AB/2	VES1	VES 2	VES3	VES4
1	731.14	165.28	81.953	57.916
2	810.71	161.4	79.151	82.786
3	867.18	127.1	85.428	101.15
4	793.21	127.28	97.639	117.75
6	523.45	128.94	109.19	140.39
8	353.15	131.15	109.01	134.82
10	216.55	120.62	99.008	128.12
12	150.77	97.509	92.834	119.39
15	108.94	77.272	81.804	101.25
20	87.531	71.064	68.769	81.546
25	71.361	61.936	65.265	72.379
30	60.842	55.703	56.705	69.582
35	53.167	44.689	52.29	68.744
40	49.299	39.478	51.14	67.665
50	42.704	31.057	53.286	61.645
60	50.529	25.901	52.026	54.887
80	144.995	17.529	43.164	43
100	48.031	17.056	46.46	31.279
125		6.3188	18.66	21.576
150		13.485	31.24	19.9
200			20.954	15.255
250			81.712	11.454
300			2.2513	

3.1.1.1 Geoelectrical aspects

The VES stations and 2D resistivity imaging traverse are shown in Fig. 8. Table 3 is the field data for VES stations. The Win-Resist modelled curve for VES 1 and VES 2 are shown in Figs. 9 and 10. The unconfined aquifer system in VES 1 lies within 0 to 11 m. Water table for hand- dug

wells (wells 6 and 7) in the vicinity of VES 1 are 9.3 and 9.4 m. These are about 2 m shallower than the base of the aquifer. In this town, as in most other communities, digging stops almost immediately after water is struck. This implies that well 6 and 7 becomes dry as water level falls below 10 m in the dry season. The unconfined aquifer unit is the sandstones facies. It is underlain between 11 m and 39.2 m by mudstone/shale facies which together with the sandstone facies constitute the confined aquifer system. A confined aquifer system is revealed from 39.2 to 72.9 m. The unconfined aquifer in the vicinity of VES 2 is from 0 to 13.4 m. Depth to water level in the hand-dug wells (13, 14, and 16) in the vicinity of VES 2 varies from 9 to 11.8 m. The modelled geoelectric section shows that the unconfined aquifer in VES 2 is from 0 to 13.4 m. The hand-dug wells dry up as water levels falls below 12 m in the dry season.

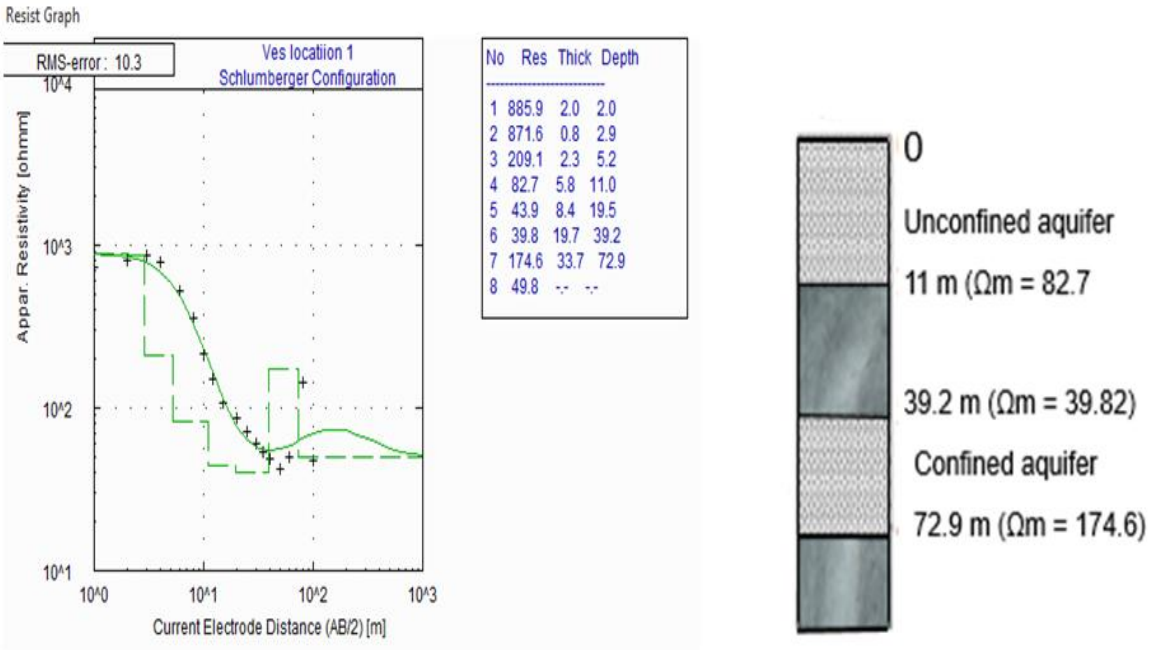

Fig. 9. 1D profile plots and geoelectric section at VES1

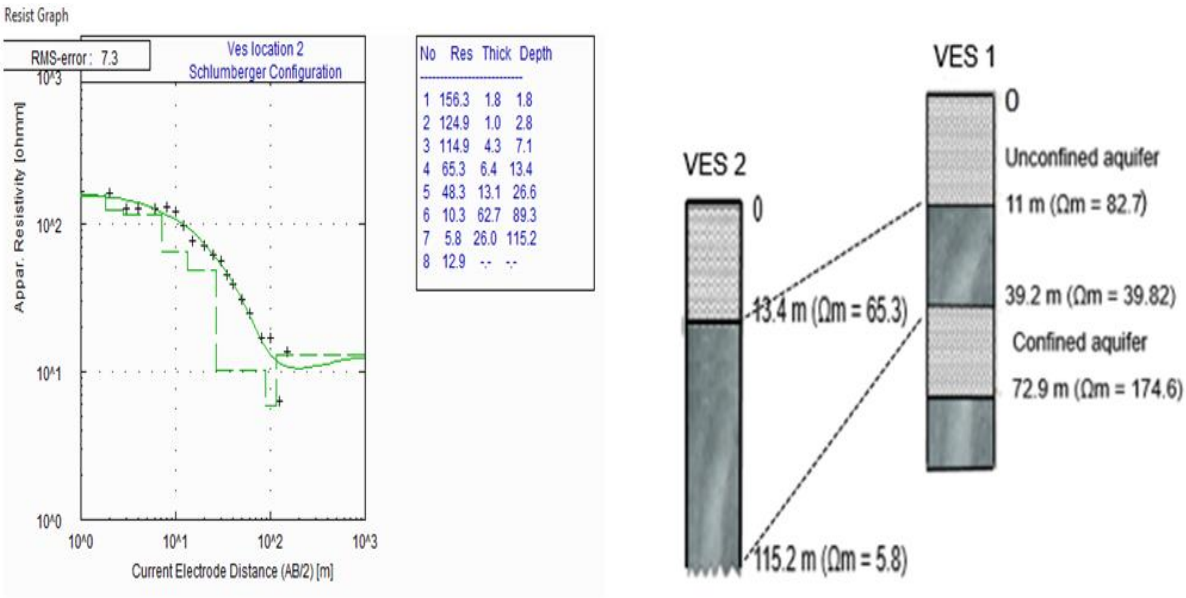

Fig. 10. 1D profile plots and geoelectric section at VES 2

Figs. 11 and 12 are Win-Resist modelled curves and geoelectric sections represent VES 3 and 4. Unconfined aquifer at VES 3 is from 0 to 5.4 m. The water level depth in hand-dug well very close to the VES is 4.9 m. it is productive throughout the year apparently because it terminated close to the base of the unconfined aquifer (5.4 m). The confined aquifer are revealed by VES 3. It lies within 45.2 and 71.3 m. The unconfined aquifer lies from 0 to 4.7 m at VES 4. The water level depth of the hand-dug well 27, around the VES station is 3.1 m. This is close to the bore of the unconfined aquifer, and the well is productive throughtout the year. One confined aquifer exists between 12.0 and 29.4 m. The resistivity imaging profile along traverse P1 and the position of VES 3 is shown in Fig. 13. The profile revealed the base of the unconfined aquifer at the position of VES 3 to be about 9.0 m. The profile did not capture the confined aquifer which begins from 45.2 m in the Win-Resist geoelectric section. The resistivity imaging profile along traverse P2, together with positon of VES 4 (Fig. 14). The profile revealed that the base of the unconfined aquifer is about 4.0 m. This is in close agreement with 4.7 m on the Win-Resist geoeletric model. The profile also capture the confined aquifer revealed on VES 4. The interval of this unit is between 12 and 30 m. This closely agrees with 12 to 29.4 m interval on the Win-resist geoelectric section. The VES data (Table 3) shows that the resistivity values vary from 48 to 227 Ωm. This supports the unconfined aquifer's high porosity (0.27- 0.42) and hydraulic conductivity (40.2 m/day).

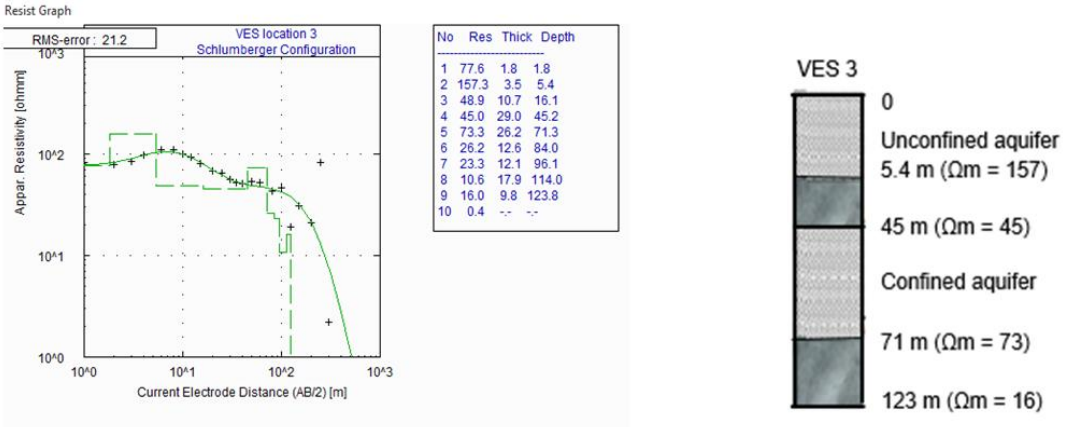

Fig. 11. 1D profile plots and geoelectric section

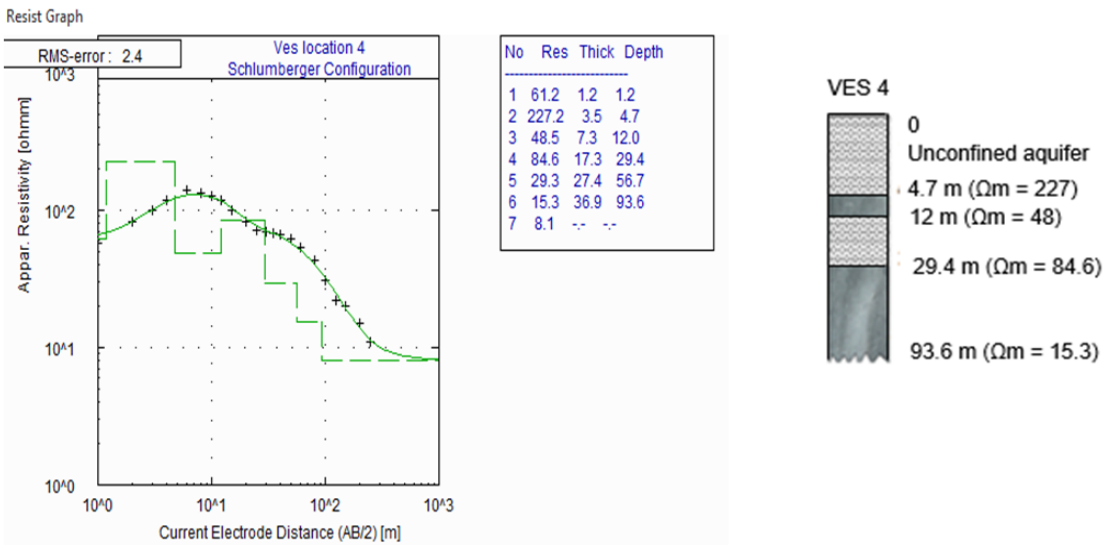

Fig. 12. 1D profile plots and geoelectric section

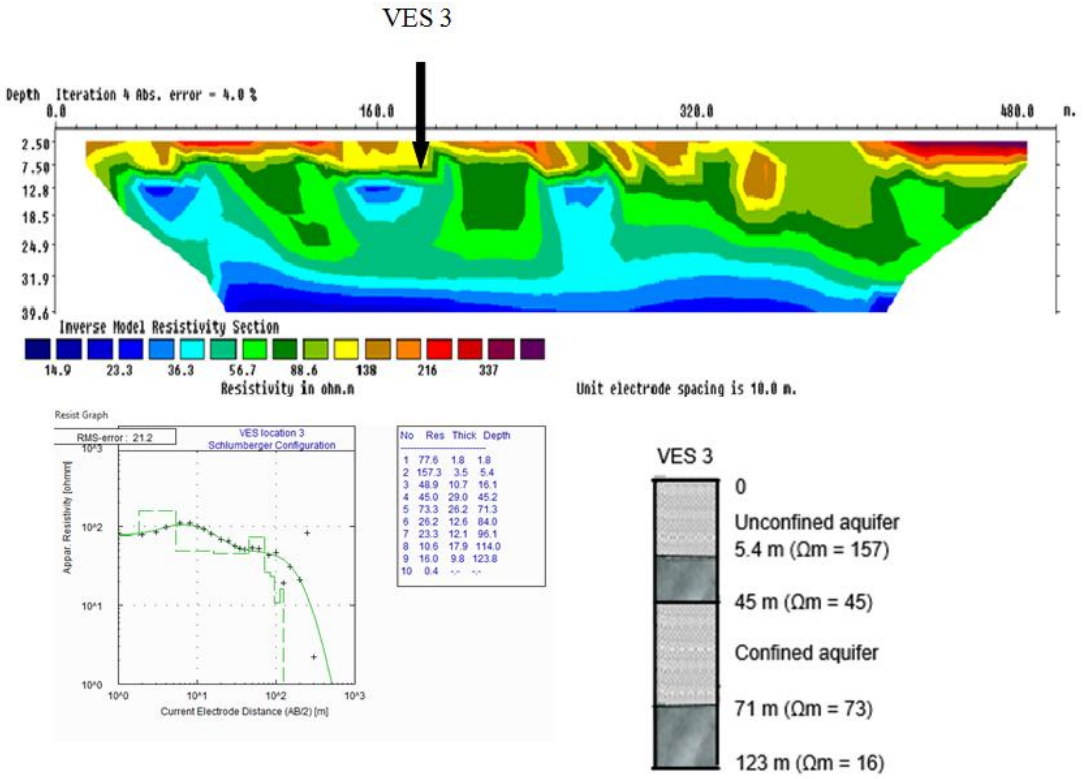

Fig. 13. 2D transverse model and VES 3

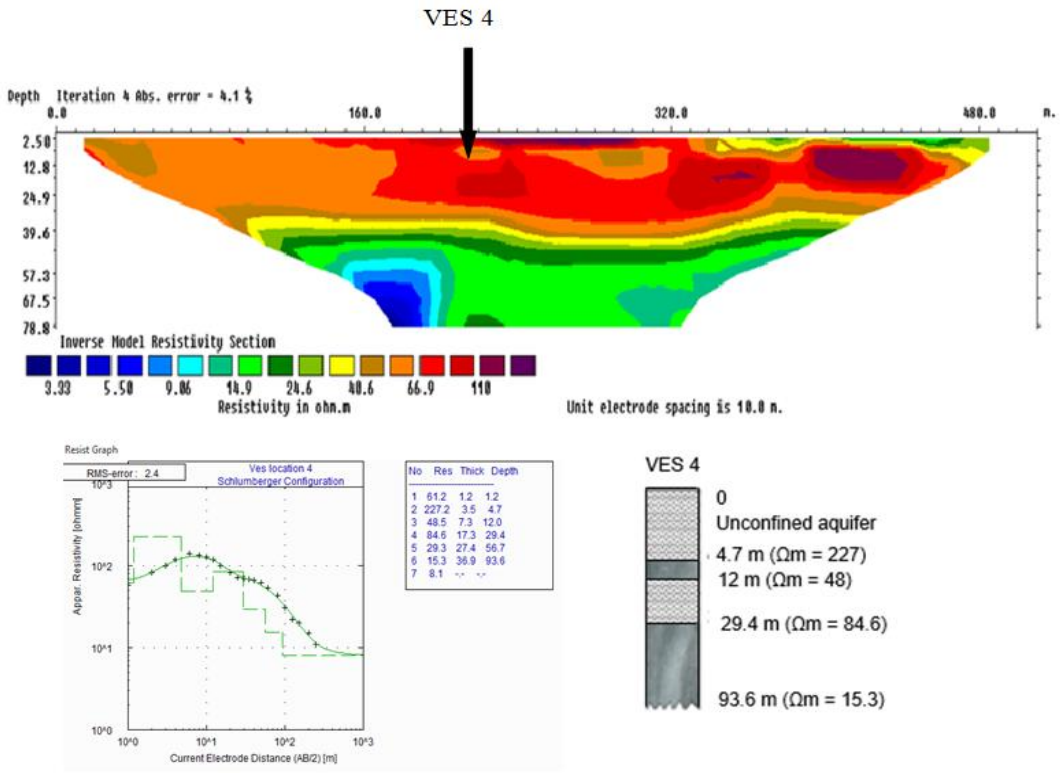

Fig. 14. 2D transverse model and VES 4

4. CONCLUSION

Surface lithological mapping of girinya and its environs revealed that the outcropping lithofacies belong to the Patti and Agbaja Formations. Empirical calculations from sieve analysis results showed that the sandstone facies have high porosity (0.27 to 0.42) and excellent hydraulic conductivity (up to 40.2 m/day) values. Observation from hand-dug wells revealed that sandstone aquifer constitute the unconfined aquifer from which water is obtained in the hand-dug wells within the town. Mapping of the hand-dug wells water level revealed one major groundwater convergence zones, two subsidiary convergence zone and one divergence zone. The wells in the vicinity of the divergence zone produce water only during the rainy season. The combination of 1D and 2D profiling show that water table is generally about 2m shallower than the base of the unconfined aquifer. The hand-dug wells therefore become dry during the dry season (continuous duration of 4 to 5 months without rainfall) when the water table falls below the base of the hand-dug wells. The 1D VES revealed that deep confined aquifers exist, (for example below 110 m in the vicinity of VES 2). The benefit of this study information that (i) hand-dug well should be dug below 32.9 m (the deepest base of the unconfined aquifer) and (ii) that boreholes should be drilled below 110 m to penetrate deep confined aquifers for sustainable groundwater supply.

COMPETING INTERESTS

Authors have declared that no competing interests exist.

REFERENCES

1. World Health Organisation. Technical notes on drinking water, sanitation and hygiene in emergencies; 2013. Available:http://www.who.int/water_sanitation_health
2. Bhattacharya PK, Patra H. A direct current geoelectric sounding. Principles and interpretations. Methods of Geo-chemistry and Geophysics. 1968;1(9):133-140.
3. Unuevho CI, Onuoha KM, Alkali YB. Direct current resistivity method for groundwater prospecting in hardrock terrains: A viable approach to providing sustainable potable water. Centre for human settlement and Urban Development Journal. 2012;3(1):1-11.
4. Helmut H, Herbert B. Dictionary of Geotechnical Engineering. 2nd Edition Springer- Verlag Berlin; 2014.
5. Jatau BS, Lazarus G, Oleka BA. Geoelectric drilling of part of Abaji and environs Abaji area council Federal Capital Territory Abuja, north central Nigeria. International Research Journal of Natural Sciences. 2013;1(2):1-10.
6. Idris-Nda A, Abubakar SI, Waziri SH, Dadi MI, Jimada AM. Groundwater development in a mixed geological terrain: A case study of Niger State, central Nigeria. Water Resources Management. 2015;8:78–87. DOI:102495/WRM150071
7. Rubin Y, Hubbard S. Hydrogeophysics, water science and technology library 50. Springer, Berlin. 2005;523.
8. Niwas S, Celik M. Equation estimation of porosity and hydraulic conductivity of Ruhrtal aquifer in Germany using near surface geophysics. Journal of Applied Geophysics. 2012;84:77–85.
9. Aizebeokhai AP. 2D and 3D geoelectrical resistivity imaging: Theory and field design. Scientific Research and Essays. 2010; 5(23):3592-3605.
10. Ratnakumari Y, Rai SN, Thiagarajan S, Kumar D. 2D electrical resisttivuty imaging for dileanation of deeper aquifers in a part of the Chandrabhaga river basin, Nagpur District, Maharashtra, India. Current Science. 2012;102:1.
11. Braide SP. Geological development, origin and energy mineral resources potential of the Lokoja Formation in the southern Bida basin. Journal of Mining and Geology. 1992;28:33–34.
12. Adeleye DR. Origin of ironstone, an example from the middle Niger Basin, Nigeria. Journal of Sedimentary Petrology. 1973;43:709-727.
13. Hazen A. Some physical properties of sands and gravels: Mass state board of health. 24th Annual Report. 1893;539-556.
14. Freeze RA, Cherry JA. Groundwater: Prentice hall Inc., Englewood Cliffs, New Jersey; 1979.
15. Vukovic´ M, Soro A. Determination of hydraulic conductivity of porous media from grain-size composition. 1st Edition, Water Resources Publications. 1992;71-84.
16. Loke M. Res2dinv version 4.08. Geoelectrical imaging 2D and 3D. instruction manual. Geotomo Software; 2018.

Available:http://www.geotomosoft.com/downloads.php

17. Allen DJ, Brewerton LJ, Coleb MA, MacDonald AM, Wagstaff SJ, Williams AT. The physical properties of major aquifers in England and wales. British Geological Survey Technical Report. WD/97/34. Environment Agency. R&D publication. 1997;312.
18. Garg SK. Soil mechanics and foundation engineering; recent developments onshore and offshore. Proc. 7th World Petroleum Congress. 2005;2:195–209.

Peer-review history:
The peer review history for this paper can be accessed here:
http://www.sciencedomain.org/review-history/26080